World Academy of Science, Engineering and Technology
International Journal of Chemical and Molecular Engineering
Vol:2, No:10, 2008

Numerical Study of Microscale Gas Flow-Separation Using Explicit Finite Volume Method

A. Chaudhuri, C. Guha, and T. K. Dutta

***Abstract*—**Pressure driven microscale gas flow-separation has been investigated by solving the compressible Navier-Stokes (NS) system of equations. A two dimensional explicit finite volume (FV) compressible flow solver has been developed using modified advection upwind splitting methods (AUSM+) with no-slip/first order Maxwell's velocity slip conditions to predict the flow-separation behavior in microdimensions. The effects of scale-factor of the flow geometry and gas species on the microscale gas flow-separation have been studied in this work. The intensity of flow-separation gets reduced with the decrease in scale of the flow geometry. In reduced dimension, flow-separation may not at all be present under similar flow conditions compared to the larger flow geometry. The flow-separation patterns greatly depend on the properties of the medium under similar flow conditions.

***Keywords*—**AUSM+, FVM, Flow-separation, Microflow.

I. Introduction

STUDIES of detailed characteristics in curved microchannels or microdevices with varying flow areas are very limited in the relatively new and exciting field of microscience and microtechnology. Understanding of fluid flow, heat transfer, mixing, and flow-separation in microdimension are quintessential for the design and optimization of various microdevices. Flow in curved microchannels finds its applications in many microsystems. Several investigators have utilized Direct Simulation Monte Carlo (DSMC) approach involving high computational cost for the prediction of hydrodynamics and heat transfer for microscale gas flows. Solution of NS system of equations along with the slip models has emerged as an alternative solution technique to deal with the miniaturization effect in slip flow regime. A significant amount of research has been carried out on analysis of fluid flow, heat transfer and application of slip models for the prediction of microscale gas flow [1-5]. Fluid flow and heat transfer in partially heated microchannels and high speed gas flow characteristics in microchannels have been presented in [6, 7]. Yan and Farouk [8] studied gas flow and mixing in a microchannel at near atmospheric conditions. Xu and Chen [9] applied DSMC method to investigate the effects of rarefaction and compressibility on the micro flow and predicted that the compressibility has significant effect on flow characteristics in the slip regime. Studies of gas flow in a straight but non-uniform (constrictions) or uniform but non-straight microchannels (bends) have been reported in [10, 11]. The results suggest that due to the complex geometry there exists extra pressure loss in these microchannels. These may be related to flow-separation around sharp corners. However, little is known about the hydrodynamics in complex flow geometries in microdimensions, and unexpected flow phenomena have been observed in microfluidic devices.

In this work, pressure driven microscale gas flow-separation phenomenon is numerically studied by solving compressible NS system of equations with no-slip/slip boundary conditions. A two dimensional explicit finite volume solver has been developed using modified advection upwind splitting methods (AUSM+) to study the flow-separation behavior in microdimensions. The developed code has been validated and tested in our previous works [6, 7, 12-14] with non-reactive and reactive microscale gas flow problems. In this paper, a comparative study with varying scale-factor of the flow geometry has been carried out taking air as the working fluid. The gas flow-separation characteristics of Air, Argon and Hydrogen gases have also been studied for similar flow conditions in the present work.

II. Problem Description

Fig. 1 illustrates the flow geometry of the test cases and Table I summarizes the parameters, height (H: z axis) and lengths (L: y axis) for all test cases. The inlet temperature for each case is 300K. Pressure is kept 1.26 atmospheres at the inlet and 1 atmosphere at the outlet. Other variables are obtained as a part of the solution at the inlet/outlet boundary for each test case. Stagnant conditions for velocities and inlet conditions for other variables are assigned as the initial conditions throughout the computational domain. Since the variation of temperature is negligible for each test case, the viscosity and thermal conductivity are calculated using Sutherland's laws at 300K.

A. Chaudhuri, presently postdoctoral researcher, INSA de Rouen, CORIA-UMR CNRS 6614, Avenue de l'Universite BP8, 76801 Saint Etienne du Rouvray, France (e-mail: arnab_chaudhuri74@yahoo.co.in, arnab.chaudhuri@coria.fr).

C. Guha (e-mail: cguhapaper@yahoo.com) and T. K. Dutta (e-mail: proftapas_dutta@yahoo.com) , Professor, Chemical Engineering Department, Jadavpur University Kolkata- 700032, India.

III. Numerical Methods

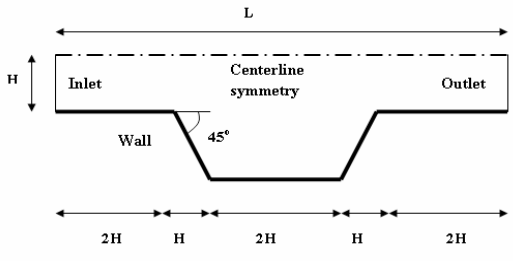

Fig. 1 Schematic of the flow geometry

TABLE I
Simulated Test Cases

Case	Fluid	H (μm)	Grid
1	Air	5	60 × 30, 60 × 40
2	Air	0.5	50 × 20, 50 × 30
3	Air	50	60 × 40
4	Argon	5	60 × 40
5	Hydrogen	5	60 × 40

Finite volume discretization of the reactive NS system of equations (conservative) for compressible flow yields a set of algebraic equations that can be solved either by explicit or implicit method. Body fitted structured meshes have been generated utilizing algebraic mapping to solve the discretized equations. The convective fluxes and pressure terms are calculated using advection upwind splitting method (AUSM+) [15, 16] at a cell interface. The diffusive fluxes are calculated using central-average representations at the interface. The source terms for momentum and energy equations are functions of viscosity and velocity gradients. These are calculated by the product of the mean value of the integrand at the control volume (CV) centre and volume of the CV. The finite volume solver relies on the accuracy and robustness of AUSM+. Symmetry, adiabatic wall and no-slip / first order Maxwell's velocity slip wall conditions are applied accordingly. The tangential momentum accommodation coefficient (σ_v) in the slip condition is taken as unity. Figs. 2 and 3 illustrate the grid dependency study for case 1 and case 2. It can be observed that there exists no significant difference among the solutions obtained from 60×30, 60×40 (case 1) and 50×20, 50×30 (case 2). The steady state solutions are achieved by explicit time marching starting from the initial conditions. The fractional change of momentum in main flow direction (y-axis) between two successive time steps is taken as the measure of convergence. The solution is considered as convergent if the maximum absolute value of the measure of convergence becomes less than 1×10^{-13} for each test case.

IV. Results and Discussion

Five test cases have been carried out to investigate the microscale gas flow-separation. Fig. 4 shows the variation of centerline Knudsen number for all test cases. It can be seen that the distribution of centerline Knudsen number for case 2 remains highest due to the lowest scale of flow geometry and the converse is true for case 3.

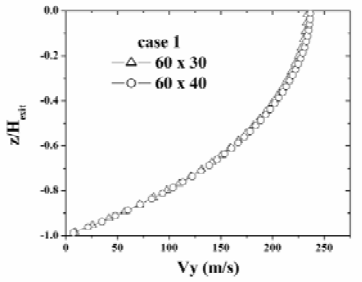

Fig. 2 Velocity (y-component) distribution at the exit plane (case 1)

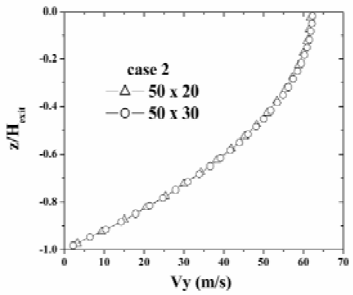

Fig. 3 Velocity (y-component) distribution at the exit plane (case 2)

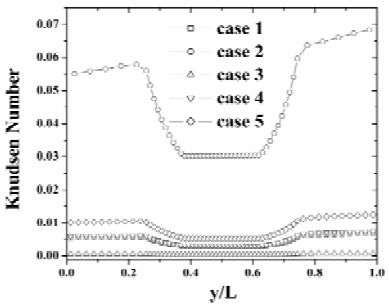

Fig. 4 Knudsen number distributions (based on centerline properties) for all cases

It has been observed that there exists no significant difference in the solution with no slip and slip wall conditions for case 1, as shown in Fig. 5, while it becomes appreciable for case 2 (Fig. 6). The results given in this paper are based on velocity slip wall conditions for all cases except case 3 where the Knudsen number remains sufficiently small to assume no slip boundary condition at the wall.

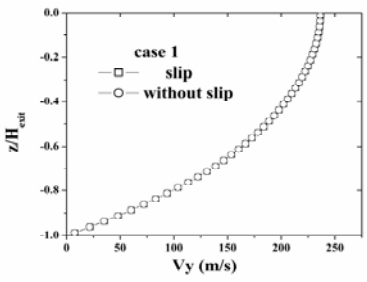

Fig. 5 Velocity (y-component) distribution at the exit plane (case 1)

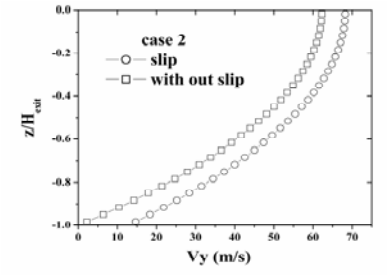

Fig. 6 Velocity (y-component) distribution at the exit plane (case 2)

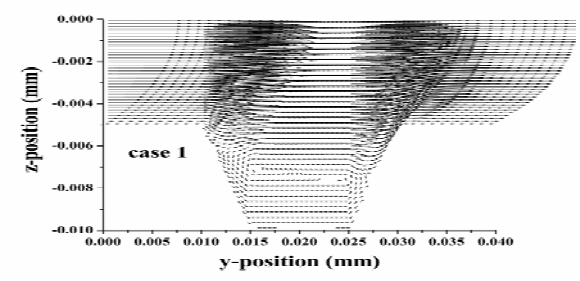

Fig. 7 Velocity vector plot for case 1

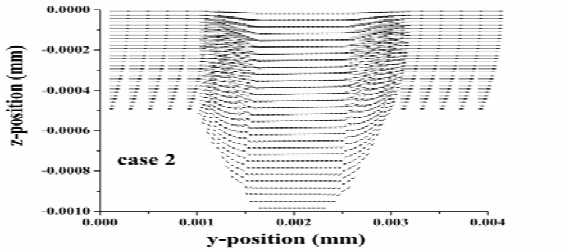

Fig. 8 Velocity vector plot for case 2

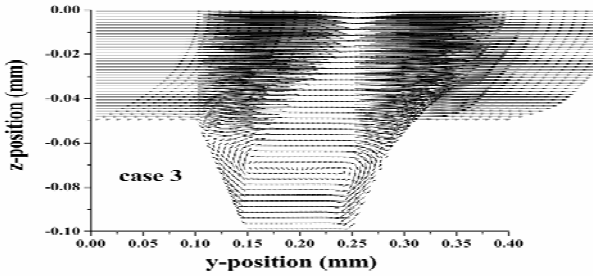

Fig. 9 Velocity vector plot for case 3

Figs. 7-9 depict velocity vector plots for case 1, 2 and 3. It is evident that two eyes of circulation exist in case 1 and those are detached from each other. On the other hand, for case 2 flow-separation is almost absent. For case 3 the scale of the flow geometry is highest. In this case the two eyes of circulation have appeared attached, closely symmetric and stronger than case 1. Fig. 10 shows that the non-dimensional pressure (centerline) distributions are also in accordance with the abovementioned flow pattern. It can be clearly observed that the non-linearity in the pressure profile gradually gets smoothened from case 2 to case 1 and then to case 3.

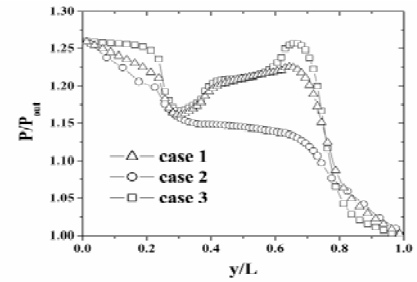

Fig. 10 Centerline non-dimensional pressure distribution for case 1-3

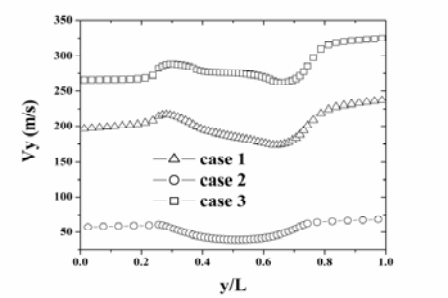

Fig. 11 Centerline velocity (y-component) distribution for case 1-3

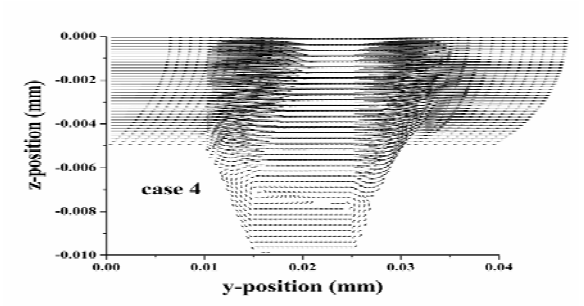

Fig. 12 Velocity vector plot for case 4

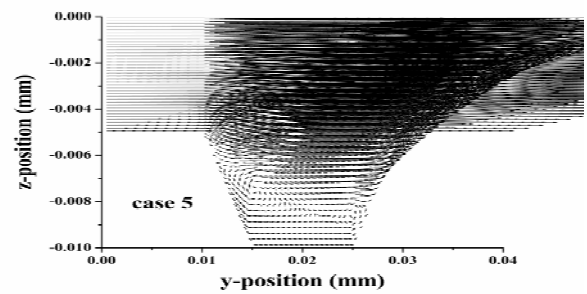

Fig. 13 Velocity vector plot for case 5

The corresponding centerline velocity (y-component) distributions are shown in Fig. 11 for case 1, 2 and 3. It can be seen that the centerline velocity (y-component) remains highest throughout for case 3 (having largest scale of flow geometry) and the reverse is predicted for case 2 (having lowest scale of flow geometry). Figs. 12 and 13 illustrate the velocity vector plots for case 4 and 5 respectively. It is interesting to note the similarity of detached circulation patterns among case 1, 4 and 5. Although the centerline pressure distribution remains closely similar for these cases (Fig. 14), the velocity for hydrogen gas remains higher than

those of Air and Argon (Fig. 15). It is also clear from Fig. 13 that the left eye of circulation becomes bigger with respect to the right eye of circulation for Hydrogen (case 5) and the right circulation moves to a little lower position than the other cases. In addition to that both circulations are stronger than those in case 1 and 4. The effects of lowest viscosity coefficient of Hydrogen (case5) and highest viscosity coefficient of Argon are, therefore, in accordance with the predicted velocity field. This is also evident from the predicted parabolic velocity (at exit plane) profiles for these cases as shown in Fig. 16. The maximum velocities at the exit plane are approximately 237 m/s, 198 m/s and 732 m/s for case 1, 4 and 5 respectively.

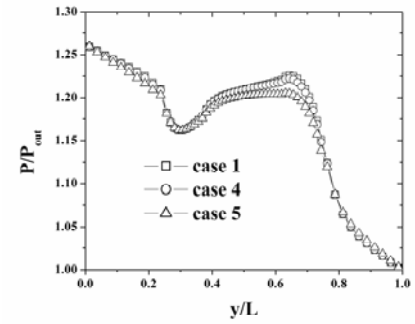

Fig. 14 Centerline non-dimensional pressure distribution for case 1, 4 and 5

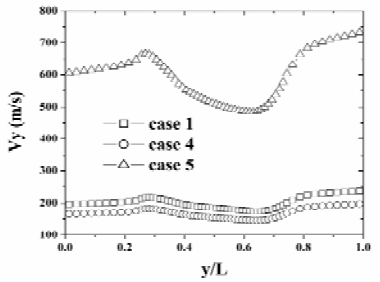

Fig. 15 Centerline velocity (y-component) distribution for case 1, 4 and 5

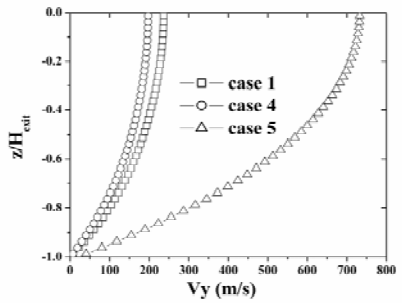

Fig. 16 Velocity (y-component) distribution at the exit plane for case 1, 4 and 5

V. Conclusion

The developed two dimensional NS solver based on finite volume method for compressible flow utilizes the central differencing scheme for the computation of diffusive flux and AUSM+ for the computation of convective flux. The first order Maxwell's velocity slip conditions are properly utilized for test cases with higher Knudsen number. In this paper, the effects of scale-factor of the flow geometry and gas species on pressure driven microscale gas flow-separation have been investigated by the developed solver. The comparative study with varying scale-factor of the flow geometry revealed that the intensity of flow-separation gets reduced with the reduction in the scale of the flow-geometry. Under similar pressure drop conditions the flow-separation does not occur in relatively smaller flow geometries as compared to the flow-separation occurring in larger flow geometries. The flow-separation patterns greatly depend on the properties of the medium.

Acknowledgment

The authors would like to acknowledge the valuable suggestions received from Mr. Nilava Sen, Faculty, Dept. of Chem. Eng. Jadavpur University.

References

[1] P. Y. Tzeng and P. H. Chen, "Numerical visualization of gaseous micro-channel flow in transition regime", *in Proc. of PSFVIP-4*, Chamonix, France, 2003.
[2] R. Raju and S. Roy, "Hydrodynamic study of high speed flow and heat transfer through a microchannel", *J. Thermophys. Heat Transfer*, vol. 19, pp.106-113, 2005.
[3] D. Jie et al., "Navier-Stokes simulation of gas flow in microdevices", *J. Micromech. Microeng*., vol. 10, pp.372-379, 2000.
[4] M. J. McNenly et al., "Slip model performance for micro-scale gas flows", *in Proc. 36th AIAA Thermophysics Conf.*, AIAA 2003-4050, pp.1-9, 2003.
[5] F. Yan and B. Farouk, "Computation of fluid flow and heat transfer in ducts using the direct simulation Monte Carlo method", *J. of Heat Transfer*, vol. 124, pp. 609-616, 2002.
[6] A. Chaudhuri et al., "Finite volume simulation of supersonic to hypersonic gas flow and heat transfer through microchannel", *Chem. Eng. Technol*., vol. 30 no. 1, pp. 41-45, 2007.
[7] A. Chaudhuri et al., "Numerical study of fluid flow and heat transfer in partially heated microchannel using explicit finite volume method", *Chem. Eng. Technol*., vol. 30 no.4, pp.425-430, 2007.
[8] F. Yan and B. Farouk, "Numerical simulation of gas flow and mixing in a microchannel using the direct simulation Monte Carlo method", *Microscale Thermophysical Eng*., vol. 6, pp. 235–251, 2002.
[9] H. Xue and S. Chen, "DSMC simulation of microscale backward-facing step flow", *Microscale Thermophysical Eng*., vol.7, pp. 69–86, 2003.
[10] Y. W. Lee and M. Wong, "Pressure loss in construction microchannels", *J. MEMS*, vol. 11, pp. 236-244, 2002.
[11] S. Y. K. Lee et al., "Gas flow in microchannels with bends", *J. Micromech. Microeng.*, vol. 11, pp. 635-644, 2001.
[12] A. Chaudhuri et al., "Numerical study of micro-scale gas flow using finite volume method", *J. of Phys. Conf. Series*, vol. 34, pp. 291-297, 2006.
[13] A. Chaudhuri et al., "Finite volume simulation of high speed combustion of acetylene-air mixture in microchannels", *Chem. Eng. Technol*., vol. 30, no.5, pp. 615-620, 2007.
[14] A. Chaudhuri et al., "Numerical study of flame acceleration in microchannel", *NanoTech 2007 Conf*., vol. 3, Chap. 3, pp. 149-152, 2007.
[15] M. S. Liou, C. J. Steffen(Jr.), "A new flux splitting method", *J. Comp. Phys*.,vol. 107, pp. 23-39, 1993.
[16] M. S. Liou, "A sequel to AUSM: AUSM+", *J. Comp. Phys*., vol. 129, pp. 364-382, 1996.